Four- dimensional climate data sets of the AMMA Special Observing Period #3

Leonard M. Druyan[1], Matthew Fulakeza[1], Patrick Lonergan[1] and Erik Noble[2]
NASA/Goddard Institute for Space Studies, NYC and
[1]Center for Climate Systems Research, Columbia University
[2]University of Colorado, Boulder CO

Abstract: Two regional models (RM3 and WRF) downscale reanalysis and FNL to a 0.5° grid over West Africa and the adjacent Atlantic Ocean. Simulations cover September 2006, the AMMA SOP-3. The presentation focuses on the characteristics of one storm system during September 10-13th..

1. Introduction

The African Monsoon Multidisciplinary Analysis (AMMA) is a concerted effort to improve our understanding of the climate of West Africa, especially the variability of precipitation systems. The goal is for this increased understanding to improve techniques of seasonal prediction of rainfall anomalies, including droughts and floods, which have a devastating socio-economic impact on very vulnerable populations of the Sahel. In addition, there is special interest in studying disturbances entering the North Atlantic from West Africa, since they are often precursors of tropical storms.

The AMMA Special Observing Period #3 (SOP-3), September 2006, employed extensive networks of ground-based and aircraft observations, supplemented by measurements from satellite-borne sensors. However, despite its ambitious scope, no field study can specify the complete space-time distribution of any of the climate variables. We have created a four-dimensional matrix of the time evolution of atmospheric conditions using regional climate models (RM3 and WRF), and validate these data sets against available meteorological data during the SOP-3. Eventually such an analysis might be improved by 4-D assimilation of observations into the integrating model output, but thus far the data sets represent dynamical downscaling of analyses to a 0.5° grid. In any case, realistic downscaling requires a model capable of simulating the important climate components of the West African monsoon (WAM). The RM3 has this capability (Druyan et al., 2006). Favorable performance of WRF has not previously been demonstrated.

The presentation shows meteorological data generated by two regional climate models, the RM3 and WRF. RM3, developed and run at CCSR/GISS, has achieved a documented and rather unique success in simulating the important mesoscale and synoptic features of the West African monsoon, including daily precipitation rates that are highly correlated in time and place with TRMM daily estimates. The Weather Research and Forecasting model (WRF) is another regional weather and climate model, which was developed at NCAR. One WRF version is currently producing operational weather forecasts over North America, but WAM applications have yet to

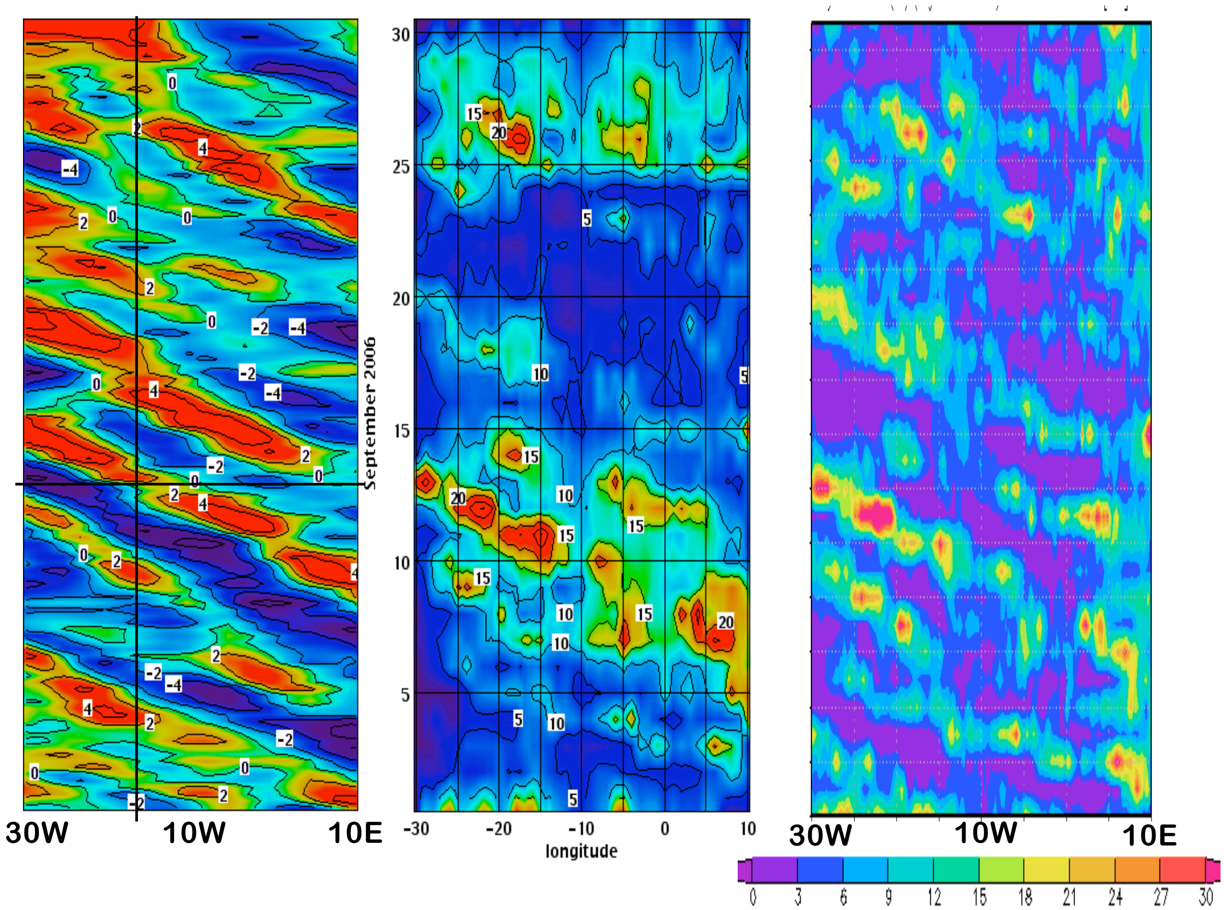

Fig. 1. Hovmöller time-longitude distributions averaged between 5-15°N for September 1-30.

Left: RM3 simulated meridional wind component at 700 mb (m s^{-1}), 4x per day. The vertical line marks the Atlantic coast of Africa and the horizontal line marks 18 UT on September 12, 2006.
Middle: RM3 simulated daily precipitation accumulations (mm).
Right: TRMM estimated daily precipitation accumulations (mm).

be discussed in the literature. The presentation shows examples from mesoscale (0.5° grid) four-dimensional data sets of evolving climate variables over West Africa for the AMMA SOP-3, September 2006, from continuous RM3 and WRF nested simulations on a grid with 0.5° spacing. Lateral boundary conditions (LBC) to drive RM3 and WRF simulations were taken four times daily from NCEP reanalyses and FNL global analyses, respectively. FNL refers to the 1°x1° observational analysis used for initial conditions in the Global Forecast System (GFS), except that FNL contains additional late data. Integrations of the RM3 are made at 28 vertical levels, within a domain extending from 20°S-35°N, 35°W-35°E, and on a grid with 0.5° spacing. The

RM3 simulation was initialized with NCEP reanalysis atmospheric conditions, SST and soil moisture for August 15, 2006 at 00 UT.

The WRF simulation described below was initialized with FNL atmospheric conditions, SSTs, and soil moisture for August 1, 2006, at 00 UT and the simulation was run until September 30, 2006 over the same domain as the RM3. The physics options used for this WRF simulation include:

- Cloud microphysics scheme: WRF Single Moment (WSM) 3-class (Skamarock et. al., 2005)
- Cumulus scheme: Kain-Fritch (Kain and Fritch, 1993)
- Surface layer scheme: Monin-Obukhov Similarity (Skamerock et. al., 2005)
- Land-surface model: Noah 4-lyr (Chen and Dudhia, 2001)
- Planetary boundary layer (PBL): Yonsei University (YSU PBL) (Skamerock et. al., 2005)
- Rapid Radiative Transfer Model (RRTM) for longwave (Mlawer et. al. 1997)
- Goddard shortwave radiative transfer (Chou and Suarez, 1994)

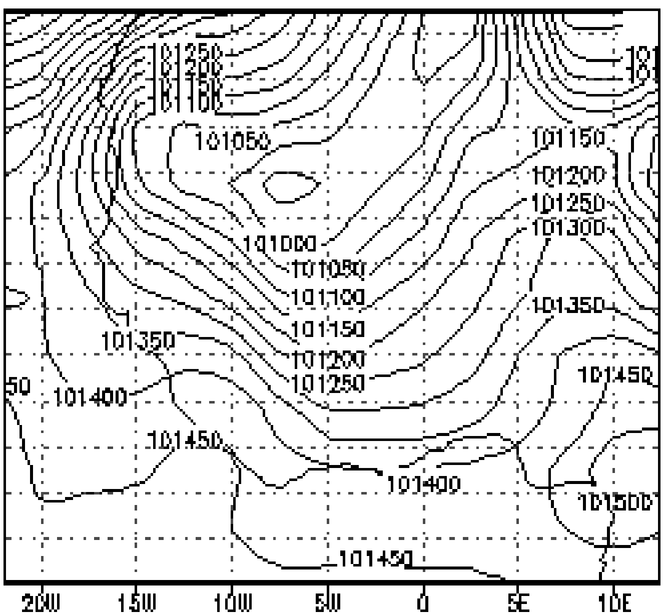

Fig. 2. NCEP reanalysis daily mean sea-level pressure distribution for Sept. 10, 2006. Isobars are labeled in Pascals. Isobar interval=50 Pascals.

Other versions of WRF using alternative components were tried, but they gave less satisfactory results, which will be reported in future publications.

2. Overview

Our colleagues at the Southern Connecticut State University have prepared an animation of the evolution of precipitation and near-surface circulation for September 2006. Precipitation is based on 3-hourly TRMM estimates and 6-hourly NCEP reanalysis circulation. Click on http://www.southernct.edu/computerscience/research/nasagiss/Animation-ModelSimulation.html/ Note specifically the evolution of the cyclonic feature over West Africa beginning September 10th. (Animations of previous RM3 simulations can be viewed at http://wamme.geog.ucla.edu/simulations.html). Fig. 1 shows

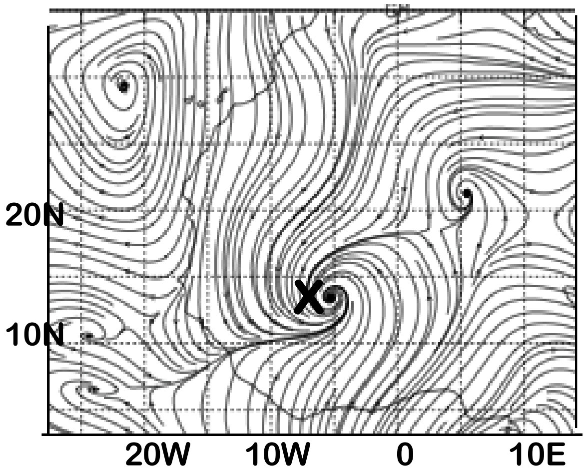

Fig. 3. Steamlines of the 925 mb circulation simulated by the RM3 for Sept. 10, 2006 at 00 UT.

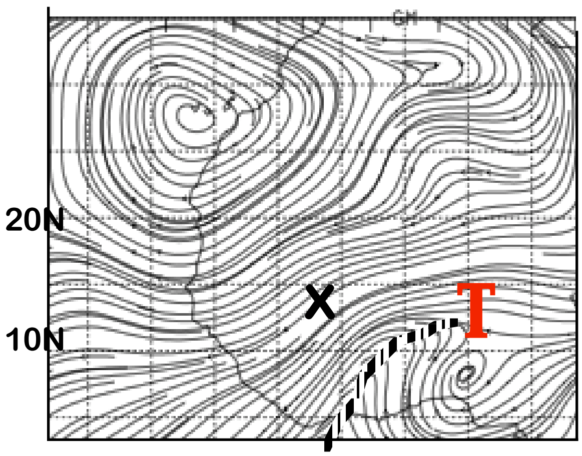

Fig. 4. Streamlines of the 700 mb circulation simulated by the RM3 for Sept. 10, 2006 at 00 UT.

Hovmöller time-longitude distributions of the meridional wind component at 700 mb (v7), 4x for each day during September 2006, and daily precipitation accumulations. In the first two panels, data are RM3 simulation results and in the third panel they are TRMM estimates. Alternating bands of negative and positive v7 show the passage of transient easterly waves, and the diagonal pattern indicates westward propagation. The easterly wave disturbance featuring the heaviest daily precipitation accumulations crossed 10°E on September 8th, reached the coast on September 12 and remained strong beyond its traversal of 30°W on September 14th. Heavy precipitation propagated westward coinciding with the sector of northerly v7 west of the moving trough line. Other westward propagating precipitation maxima are evident from both the RM3 results and TRMM estimates. In fact, the RM3 time-longitude distribution of daily precipitation accumulations is highly correlated with the

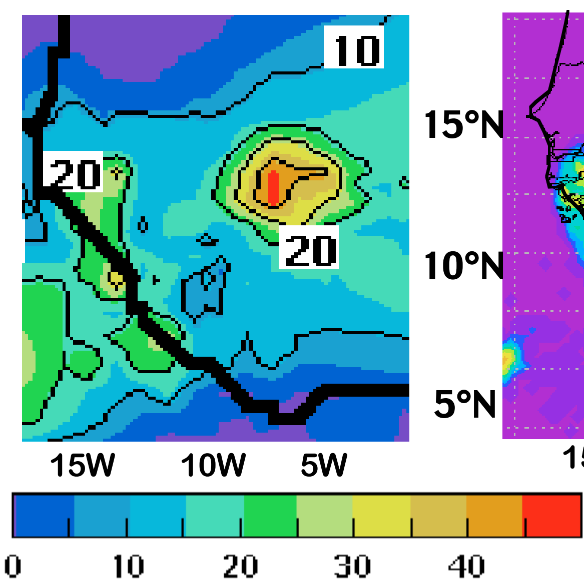

Fig. 5. RM3 simulated precipitation accumulations (mm) for Sept. 10, 2006.

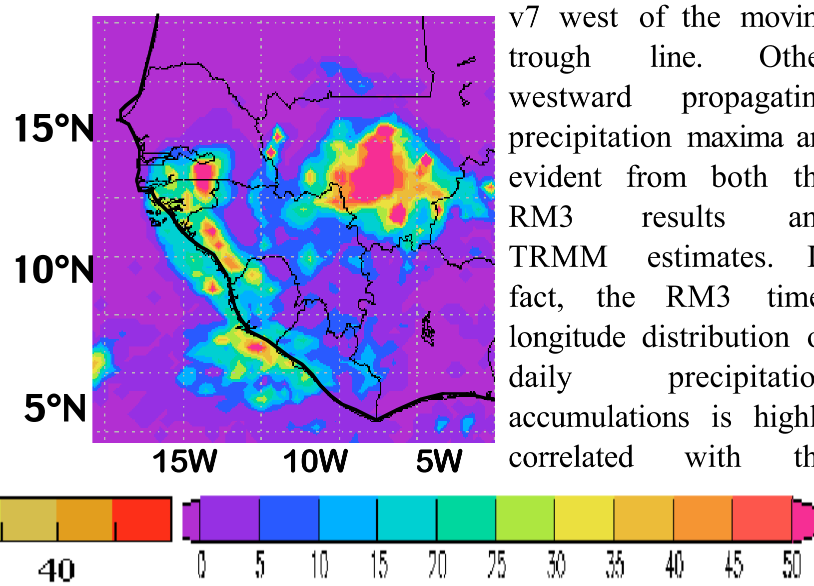

Fig. 6. TRMM estimates of precipitation accumulations (mm) for Sept. 10, 2006.

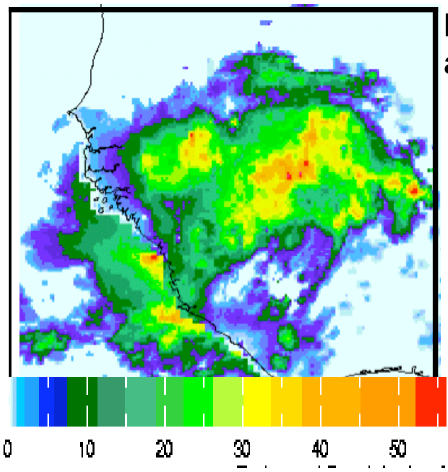

Fig. 7. FEWS estimates of precipitation accumulations (mm) for Sept. 10, 2006.

timing and location of TRMM maxima. Moreover, each diagonal precipitation swath can be matched to a corresponding pair of negative and positive v7, indicating that significant precipitation events were associated with transient easterly waves.

3. The storm of September 10-12, 2006

This African easterly wave disturbance crossed the African Atlantic coast on September 12th. Its movement and structure during the segment September 10-13 are next examined. Fig. 2 shows the reanalysis sea-level pressure distribution (SLP) for September 10, 2006, which includes a low center over 17°N, 7°W and an associated north-south trough. Fig. 3 shows the 925 mb circulation simulated by the RM3 at 00 UT on Sept. 10, 2006. The center of cyclonic circulation at 925 mb is slightly southeast of the SLP low (14°N, 5°W). The disturbance causes lower tropospheric convergence over much of West Africa, including a southwesterly monsoon flow from the Gulf of Guinea coast to the Sahel. The disturbance is associated with an easterly wave that can be discerned in the circulation at 700 mb (Fig. 4). The 700 mb trough is oriented northeast-southwest and it passes through 11°N, 0°, which is southeast of the SLP trough. The **X** on Figs, 3 and 4 marks the center of a precipitation feature discussed below.

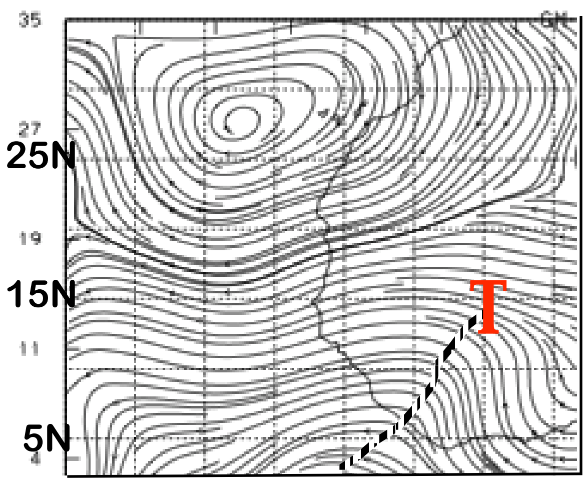

Fig. 8. Streamlines of RM3 simulated 700 mb circulation for Sept. 11, 2006 at 00 UT.

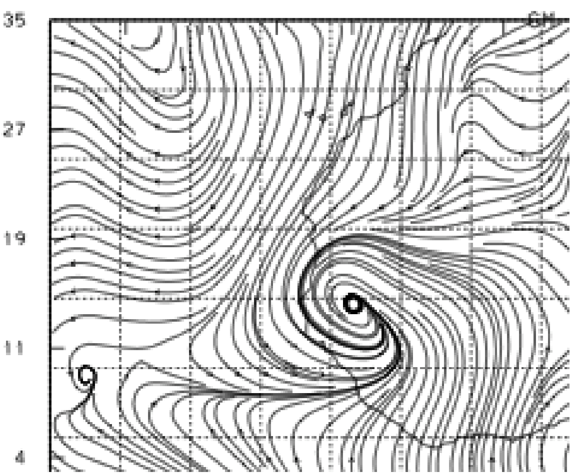

Fig. 9. Streamlines of RM3 simulated 925 mb circulation for Sept. 11, 2006 at 00 UT.

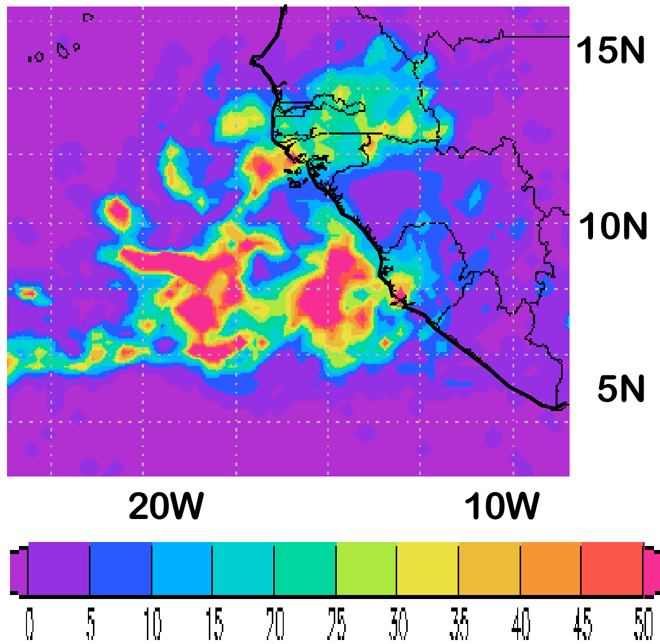

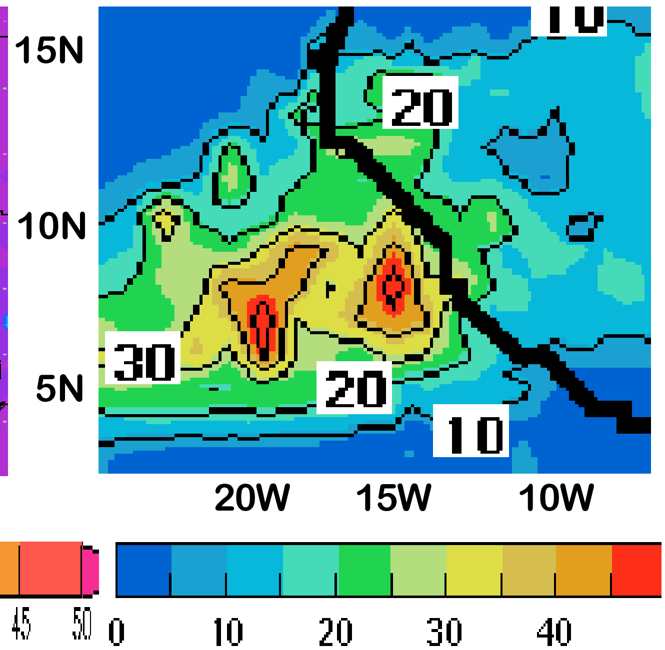

Fig. 10. (left) TRMM estimates of precipitation accumulations (mm) for Sept. 11, 2006.

Fig. 11. RM3 simulated precipitation accumulations (mm) for Sept. 11, 2006.

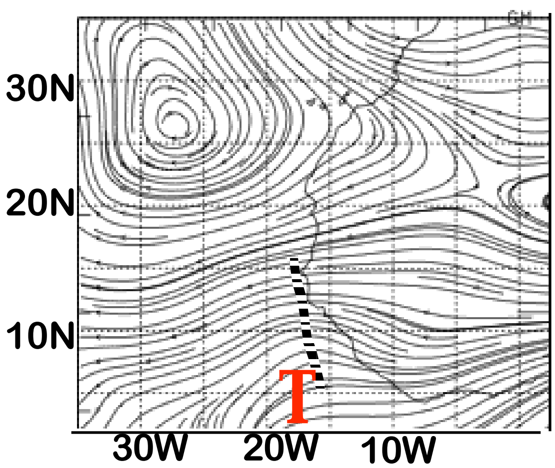

Fig. 12. RM3 simulated streamlines of the 700 mb circulation for Sept. 12, 2006 at 00 UT.

Figs. 5 and 6 show the accumulated precipitation for Sept. 10, 2006, respectively for the RM3 and based on TRMM estimates. Both representations indicate a circular rainfall maximum that overlaps the center of cyclonic circulation shown in Fig. 3, but the

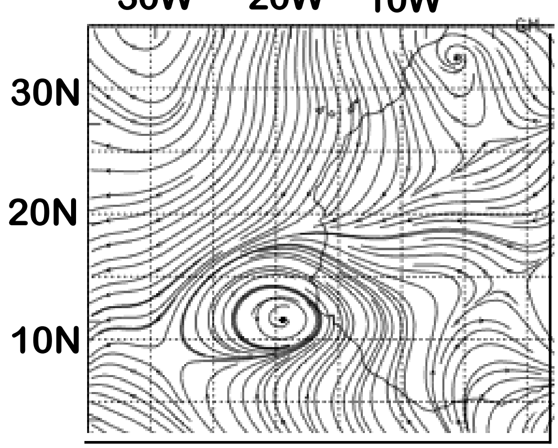

Fig. 13. RM3 simulated streamlines of the 925 mb circulation for Sept. 12, 2006 at 00 UT.

heaviest precipitation is displaced to the southwest toward the moist monsoon air mass. The circular shape of the area of heavy rainfall suggests a mesoscale convective complex. RM3 and TRMM show the same pattern of rainfall distribution, although they are not in agreement

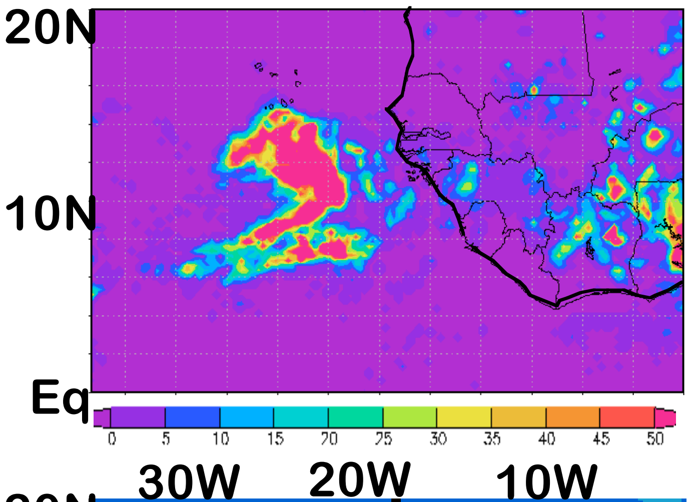

Fig. 14. TRMM estimates of precipitation accumulations (mm) for Sept. 12, 2006.

about absolute values. The RM3 simulates lower maxima, but more extensive areas of light rain. This model result is in fact closer to the corresponding FEWS distribution (Fig. 7). Nevertheless, a dearth of rain-free events within the West African ITCZ is a documented shortcoming of the RM3 (Druyan et al., 2006).

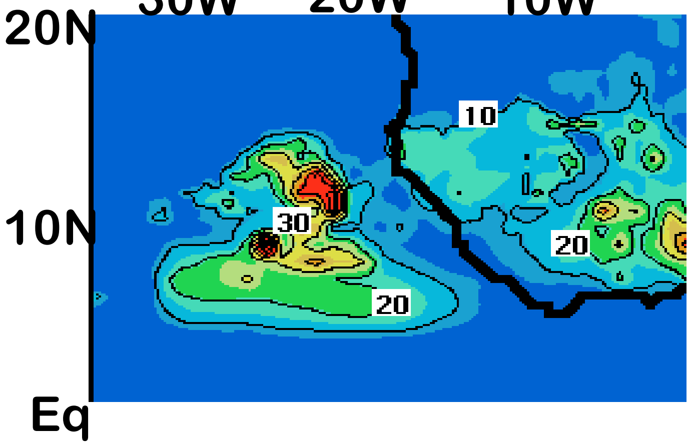

Fig. 15. RM3 simulated precipitation accumulations (mm) for Sept. 12, 2006.

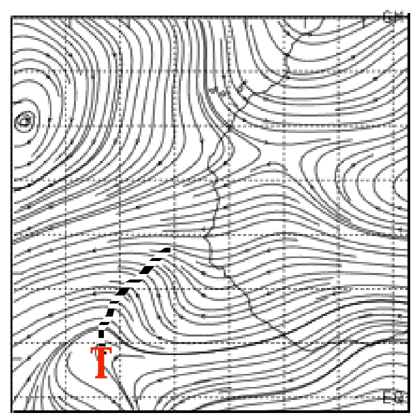

Fig. 16. RM3 simulated circulation at 700 mb for Sept. 13, 2006 at 00 UT.

By 00 UT on 11 September, the 700 mb trough (Fig. 8) has advanced westward about 5°, and the 925 mb vortex has moved about 8°. The confluence, and presumably the convergence, southwest of the vortex center has sharpened considerably and it now extends westward along 8-10°N out over the coastal waters to about 25°W (Fig. 9). Accordingly, the precipitation accumulations for Sept. 11 show a transition from the previous day (Figs. 10 and 11). In particular, the remnant of the MCC has moved in

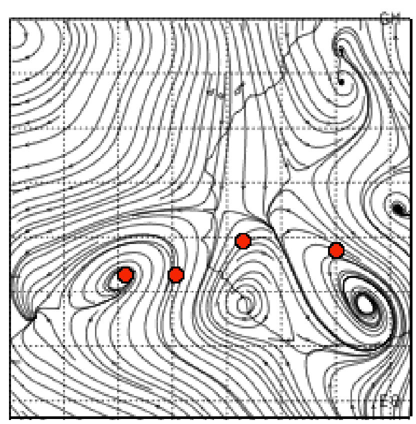

Fig. 17. RM3 simulated circulation at 925 mb for Sept. 13, 2006 at 00 UT. Red dots indicate positions of the vortex center at 00 UT for Sept. 10-13.

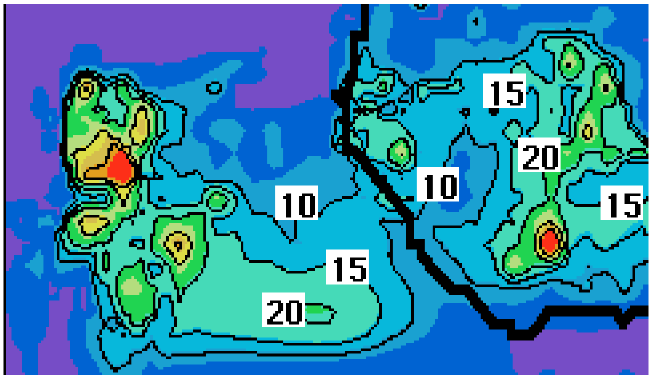

Fig, 18. RM3 precipitation accumulations for Sept. 13, 2006.

tandem with the vortex center to 13°N, 14°W, but it has weakened. Heavy precipitation has broken out along the near-surface convergence at 8°N over the coastal waters. The RM3, TRMM (Figs. 10 and 11) and FEWS show the same two precipitation maxima .

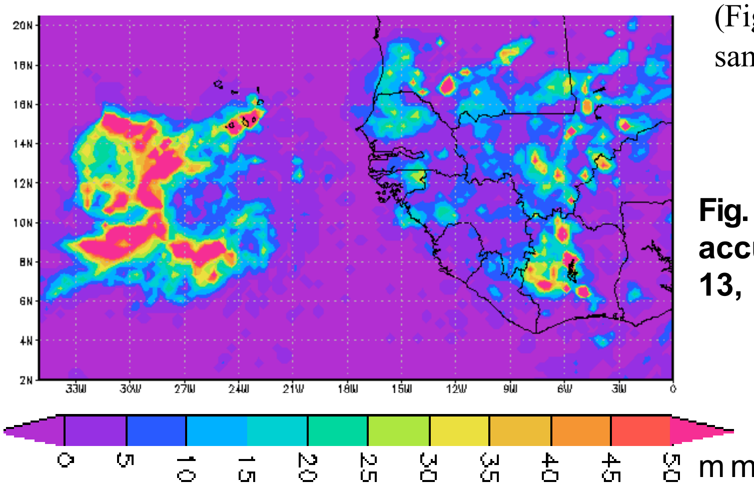

Fig. 19. TRMM precipitation accumulation estimates for Sept. 13, 2006.

The rather slow moving 700 mb trough flattens somewhat and reaches the Atlantic coast by 00 UT on September 12th (Fig. 12). The near-surface vortex is at 12°N, 20°W (Fig. 13) and has therefore shifted southward some 3°, but its zonal movement has slowed, allowing the upper trough to almost catch up. Figs. 14 and 15 show that the 8°N surface convergence zone still experiences heavy precipitation. In addition, a large comma shaped area of heavy precipitation has developed near 21°W coinciding with the low-level cyclonic vortex and the convergence zone to the north.

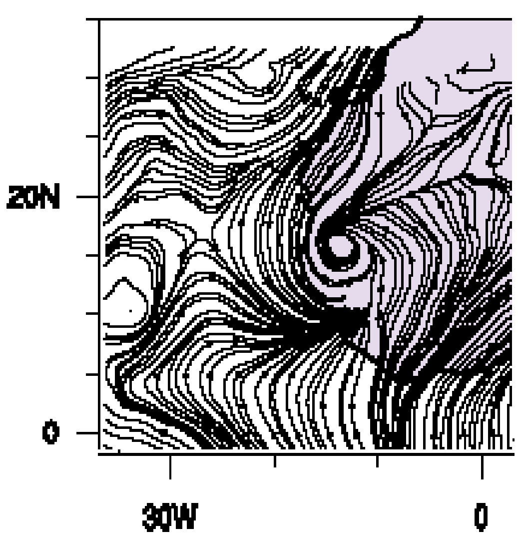

Fig. 20. WRF simulated circulation at 925 mb for Sept. 10, 2006 at 00 UT.

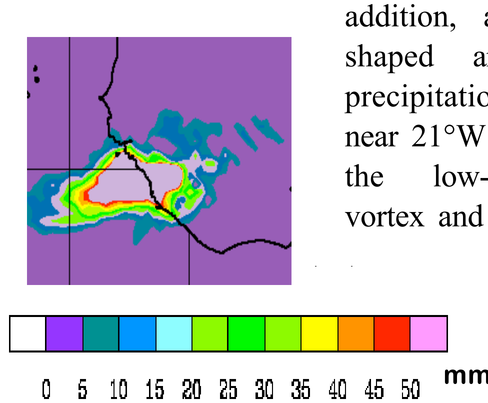

Fig. 21. WRF precipitation accumulations (mm) for Sept. 10, 2006.

Figs. 16 and 17 show the 700 mb and 925 mb circulations respectively for 00 UT on September 13th. The positions of the 925 mb center on the three previous days are also indicated in Fig. 17. The southward shift in the vortex trajectory after crossing the coastline is obvious. The NE-SW oriented trough is now vertical and has advanced some 5-8° further west in the last 24 h. The RM3 and TRMM precipitation shields (Figs. 18 and 19) wrap around the surface low from north to west to south. The extent of areas experiencing maximum rates has diminished since the previous 24 h period.

Fig. 20 shows that the September 10th position of the near-surface circulation cyclonic vortex in the WRF simulation was ahead (west) of the RM3 by some 7°. In fact it was even displaced westward of the corresponding FNL position (not shown). The WRF distribution of precipitation for September 10 (Fig.21) does not include the distinctive circular shaped maximum so prominent in Figs. 5 and 6, probably because it reflects a more advanced development, closer perhaps to the precipitation regime of September 11 (Figs. 10 and 11). Even so, the WRF maximum of accumulations in excess of 50 mm is too extreme and too broad.

Fig. 22. WRF precipitation accumulation (mm) for Sept. 12, 2006.

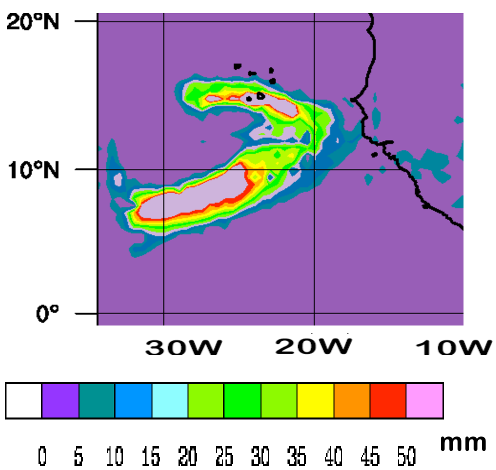

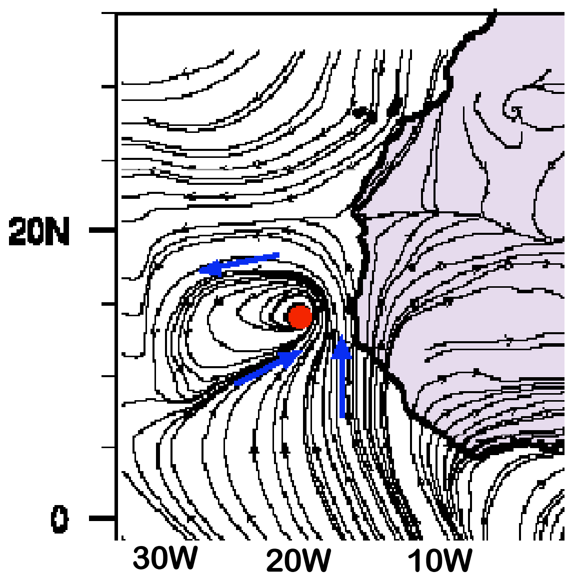

Fig. 23. WRF streamlines of the 925 mb circulation at 00 UT on Sept. 12, 2006.

WRF continues to exaggerate the area of heavy rainfall into September 11 (not shown), but by September 12, rates are more in line with observational evidence (Fig. 22). In fact, WRF simulates a comma shaped precipitation signature similar to that discussed earlier for the RM3 results and confirmed by TRMM estimates (Figs. 14 and 15). Comparison of Fig. 22 with Fig. 23 shows that the precipitation shield wraps around the southern and northern sides of the near- surface cyclonic circulation.

4. Conclusion

Both the RM3 and WRF simulate the westward propagation of an African wave disturbance across West Africa and out over the tropical eastern Atlantic during September 10-12, 2006, within the AMMA SOP-3. The disturbance was manifest by a 700 mb trough and a closed near-surface cyclonic vortex imbedded under the 700 mb northeasterlies west of the trough. Only one of six WRF model configurations that were tried gave reasonable results. In the best WRF results (reported here), the cyclonic system was displaced some 5-10° downstream of its more probable position (based on observational evidence), although the validation improved over the Atlantic. RM3 daily precipitation patterns were spatially correlated with corresponding TRMM estimates. Hovmöller time-longitude representation of model and TRMM precipitation show that this system was one of many westward propagating precipitation maximums, each presumably associated with a disturbance. Over land, a symmetrical mesoscale convective system developed under the western flank of the 700 mb trough, slightly southwest of the near-surface cyclonic center. As the AEW approached the Atlantic coast, the heaviest precipitation shifted southward, concentrating along lines of low level circulation convergence associated with the ITCZ. As it crossed the coast of Africa into the Atlantic, the near- surface cyclonic center also moved to a more southerly trajectory and slowed enough to eventually become situated directly under the 700 mb trough. Results suggest that the near- surface cyclonic vortex was drawn toward the maritime area of greatest moist convective activity.

Acknowledgements: This research was supported by NSF grant ATM-0652518, NASA grant NNX07A193G and by the NASA Climate and Earth Observing System Program. E. Noble is a Fellow of the NASA Graduate Student Researchers Program. The animations of precipitation and 925 mb circulation, accessible via the links given in Section 2, were facilitated by Dr. John DaPonte, Munhutu Paidemwoyo and Bruno Nader (all of SCSU) and Ruben Worrell of GISS. TRMM data used in this study were acquired using the GES-DISC Interactive Online Visualization ANd aNalysis Infrastructure (Giovanni) as part of the NASA's Goddard Earth Sciences (GES) Data and Information Services Center (DISC). NCEP reanalysis data used in this study were obtained on-line from the NOAA/Earth System Research Laboratory (Physical Sciences Division). FEWS data sets were created at the NOAA Climate Prediction Center and made available on-line by the International Research Institute for Climate Prediction of Columbia University.

References

Druyan L, Fulakeza M, Lonergan P. 2006. Mesoscale analyses of West African summer climate: focus on wave disturbances. *Climate Dynamics* **27**: 459-481.

Chen, F., and J. Dudhia, 2001: Coupling an advanced land-surface/ hydrology model with the Penn State/ NCAR MM5 modeling system. Part I: Model description and implementation. *Mon. Wea. Rev*., **129**, 569–585.

Chou M.-D., and M. J. Suarez, 1994: An efficient thermal infrared radiation parameterization for use in general circulation models. *NASA Tech. Memo*. *104606*, 3, 85pp.

Kain, J. S., and J. M. Fritsch, 1993: Convective parameterization for mesoscale models: The Kain-Fritcsh scheme, *The Representation of Cumulus Convection in Numerical Models*, K. A. Emanuel and D.J. Raymond, Eds., Amer. Meteor. Soc., 246 pp.

Mlawer, E. J., S. J. Taubman, P. D. Brown, M. J. Iacono, and S. A. Clough, 1997: Radiative transfer for inhomogeneous atmosphere: RRTM, a validated correlated-k model for the long-wave. *J. Geophys. Res*., **102** (D14), 16663–16682.

Skamarock, W. C. et al., 2005: A description of the advanced research WRF version 2. *NCAR Technical Note*, *June 2005; revised January 2005*.